MDD Longitudinal conhect; RS fmri matrixes

2024-03-20

Methods

fMRI data were preprocessed using fmriprep : Anatomical data preprocessing A total of 3 T1-weighted (T1w) images were found within the input BIDS dataset. Each T1w image was corrected for intensity non-uniformity (INU) with N4BiasFieldCorrection (Tustison et al. 2010), distributed with ANTs 2.5.0 (Avants et al. 2008, RRID:SCR_004757). The T1w-reference was then skull-stripped with a Nipype implementation of the antsBrainExtraction.sh workflow (from ANTs), using OASIS30ANTs as target template. Brain tissue segmentation of cerebrospinal fluid (CSF), white-matter (WM) and gray-matter (GM) was performed on the brain-extracted T1w using fast (FSL (version unknown), RRID:SCR_002823, Zhang, Brady, and Smith 2001). An anatomical T1w-reference map was computed after registration of 3 T1w images (after INU-correction) using mri_robust_template (FreeSurfer 7.3.2, Reuter, Rosas, and Fischl 2010). Volume-based spatial normalization to one standard space (MNI152NLin2009cAsym) was performed through nonlinear registration with antsRegistration (ANTs 2.5.0), using brain-extracted versions of both T1w reference and the T1w template. The following template was were selected for spatial normalization and accessed with TemplateFlow (23.1.0, Ciric et al. 2022): ICBM 152 Nonlinear Asymmetrical template version 2009c [Fonov et al. (2009), RRID:SCR_008796; TemplateFlow ID: MNI152NLin2009cAsym].

Functional data preprocessing For each of the 3 BOLD runs found per subject (across all tasks and sessions), the following preprocessing was performed. First, a reference volume was generated, using a custom methodology of fMRIPrep, for use in head motion correction. Head-motion parameters with respect to the BOLD reference (transformation matrices, and six corresponding rotation and translation parameters) are estimated before any spatiotemporal filtering using mcflirt (FSL , Jenkinson et al. 2002). The BOLD reference was then co-registered to the T1w reference using mri_coreg (FreeSurfer) followed by flirt (FSL , Jenkinson and Smith 2001) with the boundary-based registration (Greve and Fischl 2009) cost-function. Co-registration was configured with six degrees of freedom. Several confounding time-series were calculated based on the preprocessed BOLD: framewise displacement (FD), DVARS and three region-wise global signals. FD was computed using two formulations following Power (absolute sum of relative motions, Power et al. (2014)) and Jenkinson (relative root mean square displacement between affines, Jenkinson et al. (2002)). FD and DVARS are calculated for each functional run, both using their implementations in Nipype (following the definitions by Power et al. 2014). The three global signals are extracted within the CSF, the WM, and the whole-brain masks. Additionally, a set of physiological regressors were extracted to allow for component-based noise correction (CompCor, Behzadi et al. 2007). Principal components are estimated after high-pass filtering the preprocessed BOLD time-series (using a discrete cosine filter with 128s cut-off) for the two CompCor variants: temporal (tCompCor) and anatomical (aCompCor). tCompCor components are then calculated from the top 2% variable voxels within the brain mask. For aCompCor, three probabilistic masks (CSF, WM and combined CSF+WM) are generated in anatomical space. The implementation differs from that of Behzadi et al. in that instead of eroding the masks by 2 pixels on BOLD space, a mask of pixels that likely contain a volume fraction of GM is subtracted from the aCompCor masks. This mask is obtained by thresholding the corresponding partial volume map at 0.05, and it ensures components are not extracted from voxels containing a minimal fraction of GM. Finally, these masks are resampled into BOLD space and binarized by thresholding at 0.99 (as in the original implementation). Components are also calculated separately within the WM and CSF masks. For each CompCor decomposition, the k components with the largest singular values are retained, such that the retained components' time series are sufficient to explain 50 percent of variance across the nuisance mask (CSF, WM, combined, or temporal). The remaining components are dropped from consideration. The head-motion estimates calculated in the correction step were also placed within the corresponding confounds file. The confound time series derived from head motion estimates and global signals were expanded with the inclusion of temporal derivatives and quadratic terms for each (Satterthwaite et al. 2013). Frames that exceeded a threshold of 0.5 mm FD or 1.5 standardized DVARS were annotated as motion outliers. Additional nuisance timeseries are calculated by means of principal components analysis of the signal found within a thin band (crown) of voxels around the edge of the brain, as proposed by (Patriat, Reynolds, and Birn 2017). All resamplings can be performed with a single interpolation step by composing all the pertinent transformations (i.e. head-motion transform matrices, susceptibility distortion correction when available, and co-registrations to anatomical and output spaces). Gridded (volumetric) resamplings were performed using nitransforms, configured with cubic B-spline interpolation.

Functional connectomes were created following the Automatic Atlas Labeleing (AAL) in 112 regions. Pearson Correlation between each of brain regions was defined as the adjacency matrix weight. Global metrics, including global efficiency, local efficiency, smallworldness, clustering coefficient and characterstic path length were computed using R, over a range of sparsities from 10% to 50%, by steps of 1%. The area under the curve for each of the global metrics was chosen for the statistical analysis.

Statistical analysis were performed in R. Linear mixed model were used, with random effects for subject identification, and age, sex as covariates. Type II anova were used to fit the model.

MDD

Computing global_eff

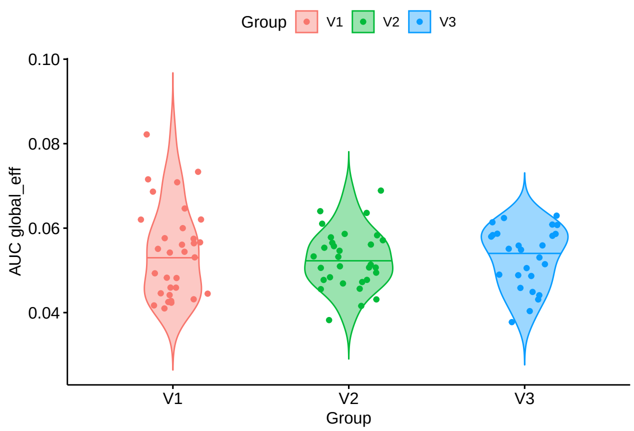

Predictors	Estimates	CI	p
(Intercept)	0.05	0.05 – 0.06	<0.001
Group [V2]	-0.00	-0.01 – 0.00	0.512
Group [V3]	-0.00	-0.01 – 0.00	0.619
age	0.00	-0.00 – 0.00	0.166
sex [H]	-0.00	-0.01 – 0.00	0.101
Observations	89		
R2 / R2 adjusted	0.066 / 0.022		

Computing local_eff

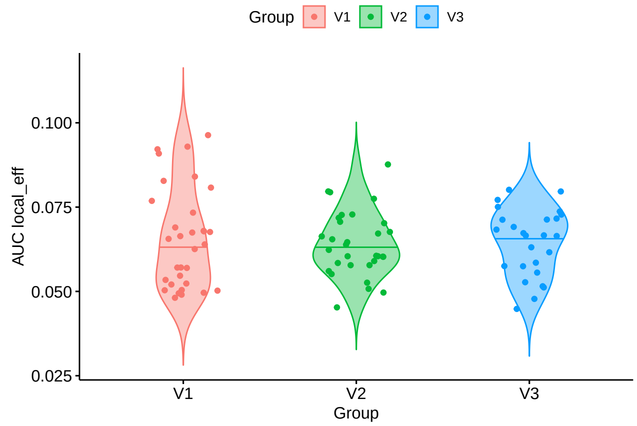

Predictors	Estimates	CI	p
(Intercept)	0.06	0.05 – 0.07	<0.001
Group [V2]	-0.00	-0.01 – 0.00	0.713
Group [V3]	-0.00	-0.01 – 0.01	0.814
age	0.00	-0.00 – 0.00	0.151
sex [H]	-0.00	-0.01 – 0.00	0.311
Observations	89		
R2 / R2 adjusted	0.043 / -0.003		

Computing characteristic_path

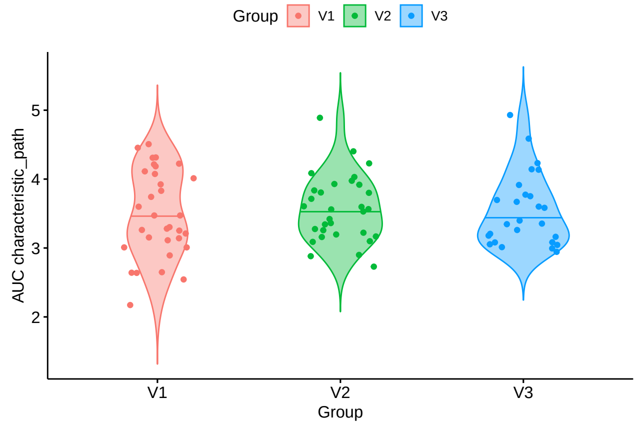

Predictors	Estimates	CI	p
(Intercept)	3.61	3.22 – 4.00	<0.001
Group [V2]	0.05	-0.22 – 0.32	0.731
Group [V3]	0.04	-0.24 – 0.32	0.789
age	-0.00	-0.01 – 0.00	0.173
sex [H]	0.28	0.05 – 0.51	0.018
Observations	89		
R2 / R2 adjusted	0.094 / 0.051		

Computing clust_coeff

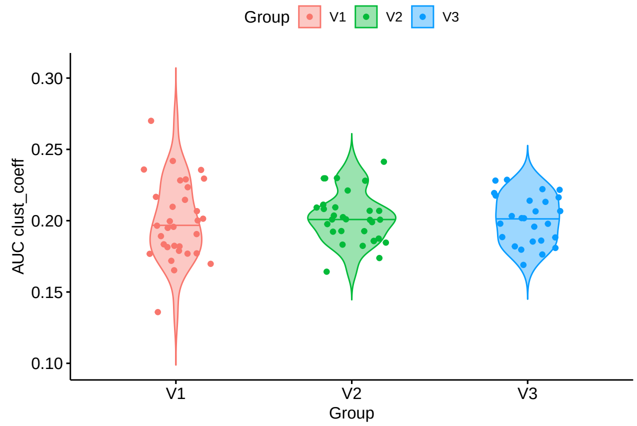

Predictors	Estimates	CI	p
(Intercept)	0.20	0.18 – 0.21	<0.001
Group [V2]	0.00	-0.01 – 0.01	0.675
Group [V3]	0.00	-0.01 – 0.01	0.796
age	0.00	-0.00 – 0.00	0.684
sex [H]	0.00	-0.01 – 0.01	0.412
Observations	89		
R2 / R2 adjusted	0.011 / -0.036		

Computing smallworldeness

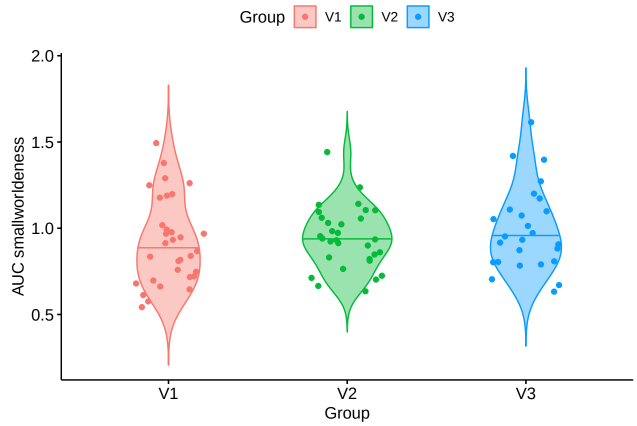

Predictors	Estimates	CI	p
(Intercept)	0.81	0.65 – 0.97	<0.001
Group [V2]	0.02	-0.09 – 0.13	0.683
Group [V3]	0.08	-0.04 – 0.19	0.197
age	0.00	-0.00 – 0.00	0.304
sex [H]	0.11	0.01 – 0.20	0.026
Observations	89		
R2 / R2 adjusted	0.082 / 0.038		